International Journal of Occupational Safety and Health

ISSN: 2091-0878 (Online) ISSN: 2738-9707 (Print)

Short Communication

Ergonomic design of noseless bicycle saddle using UPVC/Silica-Aerogel

Govindaraj P[1], Sudheep SK[2]

[1] Assistant Professor (Selection Grade), Department of Mechanical Engineering, PSG College of Technology, Coimbatore-641004, Tamil Nadu, India

[2] Graduate Student (Master of Science), Department of Industrial and Systems Engineering, Northern Illinois University, DeKalb-60115, Illinois, USA

Corresponding author:

Dr. Govindaraj P,
Assistant Professor (Selection Grade),
Department of Mechanical Engineering,
PSG College of Technology,
Coimatore-641004, Tamil Nadu, India.
E-mail: pgr.mech@psgtech.ac.in
Phone number: +91 9894036278
ORCID ID: https://orcid.org/0000-0002-2761-4091

Date of submission: 27.03.2023
Date of acceptance: 02.06.2024
Date of publication: 01.07.2024

Conflicts of interest: None
Supporting agencies: None
DOI: https://doi.org/10.3126/ijosh.v14i3.53597

ABSTRACT

Introduction: During cycling, most of people suffer from perineal pain due to the pressure acting on the perineal area by the nose of the seat. Also, Unsupported sitting on the saddle in a forward bending posture for a longer time induces low back pain (LBP) among cyclists. So, this paper presents the design of a noseless bicycle seat with a backrest using UPVC/Silica-Aerogel.

Methods: This seat is designed as per the anthropometric dimensions of human body. Various parameters such as Lumbar position, seat tilt angle, seat position, backrest angle, seat height, backrest height, seat and backrest width are considered and the optimal value is determined while designing. The material chosen for the base of seat is UPVC/Silica- Aerogel composite and the cushioning material is chosen as polyurethane foam. The design is executed in 3D modelling software and validated using FEA Package Ansys Workbench 2022 R2.

Results: The maximum stresses induced in the newly proposed material UPVC/Silica-Aerogel (4.41MPa) is lesser than its yield strength (59 MPa). The maximum anterior stress of noseless seat is found out to be 24.5 kPa which is lower than that of the saddle with nose (41 kPa).

Conclusion: As the anterior stress of noseless seat is lesser, the perineal pressure of cyclists is greatly reduced and this decreases the health problems associated with the perineal pressure. Also the backrest of the seatpan enhances the supporting of back muscles and reduces LBP among cyclists.

Keywords: Noseless seat, Perineal pressure, Unsupported sitting, UPVC/Silica-Aerogel

Introduction

The male anthropometry might influence the bicycle seat pressure and it is advisable to use male anatomy and male anthropometric data for most of the measurements while designing the bicycle seat.[1] The saddle with nose induce higher perineal pressure which in turn causes various sexual health problems. In order to reduce the pressure to the perineum of the cyclists, a saddle without a narrow protruding nose is advisable.[2]

LBP is reduced when the tensile forces on the lumbo-sacral spine is reduced. This is achieved when a forward or anterior pelvic tilt (APT) of the cyclist's pelvis is favored. An adjustment of the saddles by inclining the saddle anteriorly by 3^0 to 9^0, resulted in the reduction of LBP in 80% of the cyclists.[3] The back is subjected to various positions while cycling which in turn causes pain in the lower back among the cyclists. The introduction of a back rest is the solution to eliminate this problem. The back rest's height should be approximately half of the sitting shoulder's height and this information should be taken into account while designing backrest.[4]

The lumbar spine resembled similar to the lumbar

curve of a person standing when the backrest angle was inclined 100° to the seat pan. Also, the forward tilting of seat can prevent the flattening or kyphosis of the lumbar spine. A relaxed posture is provided when the forward tilted seat opens the angle between the upper torso and the hip.[5] The anthropometric data of the population should be focused for the purpose of designing human utilities.[6,7] The flat surfaced saddles showed a more uniform pressure distribution with less pressure on the anterior part and more on the posterior part compared with the saddle with a perineal hole.[8]

In order to overcome the drawbacks of existing construction materials more ductile, robust and durable materials are needed for bridges, buildings and other infrastructure. Therefore, an innovative system is needed to improve the performance. To ease the situation, Unplasticized polyvinyl chloride (UPVC) tubes are used as a confining material and their performance was evaluated experimentally by testing the UPVC confined cylinders. The result showed that when compared to the unconfined levels the UPVC confinement increased the strength, energy absorption and ductility.[9]

The effects of Silica Aerogels on thermal, mechanical, and acoustical characteristics when mixed with UPVC. The tensile properties, hardness, softening temperature, thermal conductivity, impact strength, sound absorption, and sound transmission loss are tested and evaluated for the prepared UPVC/Silica-Aerogel composites. The results confirmed that when adding silica aerogel to the UPVC, the hardness, tensile strength, elastic modulus and softening temperature are increased.[10] The use of UPVC/Silica-Aerogel for bicycle seat has not been explained and evaluated in any of the journals at present. The idea here is to use the UPVC/Silica-Aerogel as a material for the seat pan padding. The primary objective of the paper is to design a noseless bicycle seat with attached backrest using UPVC/Silica-Aerogel and to analyze the design feasibility and anterior saddle pressure.

Methods

A saddle with flat surface is chosen the flat surfaced saddles showed a more uniform pressure distribution with less pressure on the anterior part compared with the saddle with a perineal hole or cut out design. The 3D model of the noseless flat surfaced saddle is illustrated in figure 1.

All dimensions in mm

Figure 1: 3D model of Seat pan

The 20 mm thickness of the seat pan is split into two parts. The lower part is the padding of the saddle and the upper portion represents the cushioning of the saddle. The anthropometric dimensions considered for design of bicycle saddle are lower back – knee length, hip breadth, sit bone width, sitting shoulder height and chest breadth.

For Seat length, the Lower back – knee length is considered for 95th percentile men for domestic seats (non- bicycle seat) which is 642 mm. But for bicycle the seat length should be smaller than the lower back-knee length. The average bicycle seat length is 250 to 270 mm (with nose). For noseless seat the length should be 130 mm.[11]

Hip width for 95th percentile men should be considered for the design of domestic seats (non-bicycle seat). But for bicycle seat the sit bone (ischial tuberosity) width should be considered. The average sit bone width for men is 100 to 140 mm and 110 to 150 mm for women.[7] The seat should accommodate the person with lowest to highest sit bone width. So sit bone width of 150 mm should be considered for the design. Further 20 mm is added as addendum. So totally the seat width is 170 mm as shown in figure 2.

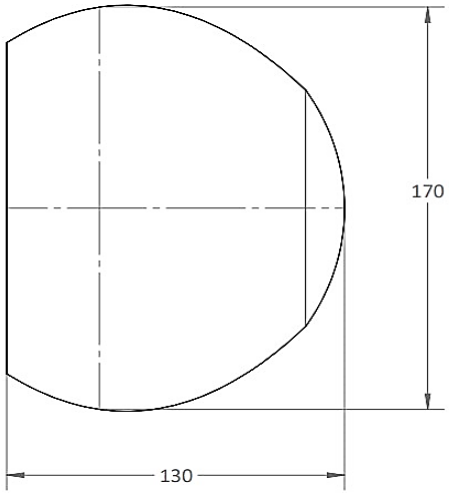

Figure 2: Proposed Seat design

If the saddle width exceeds beyond 170 mm then it leads to unstability and the thigh muscles would hit the seat edge and causes friction between thigh muscle and the seat edge.[12] Excessive thickness of bicycle seat increases the thigh pressure, whereas very low thickness of seat leads to the failure of seat by deformation when cyclists sit on the seat. So, the ideal thickness (padding and cushion) of seat is 20 to 30 mm. The padding thickness is chosen as 8.5 mm and the cushion thickness is chosen as 11.5 mm resulting to a total thickness of 20 mm.

A forward anterior tilt of the seat pan from 3^0 to 5^0 promotes a very slight forward slumped position which in turn, resulted in improvement in the incidence and magnitude of Low Back Pain in 70% of the cyclists.[13] For our design, the seat pan is tilted anteriorly to an angle of 3.75^0. To support this a supporting rod bent over 3.75^0 is attached to the base of the seat. The seat pan is fixed to the supporting rod with the help of the fixture attached to the inclined part of the rod as shown in figure 3. The supporting rod is then fixed to the seat post using the rod base and it helps to move the seat forward and backward to adjust the distance between the seat and the handlebar. The distance between the handlebar and the seat post is decided based on the grip reach (forward reach) distance of the arm.[14]

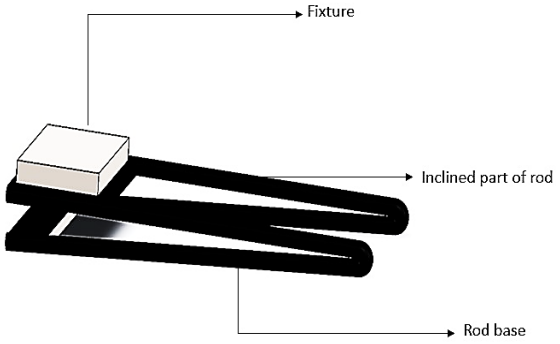

Figure 3: 3D model of the supporting rod

The seat post should be placed in such a way that it should accommodate 5th percentile women to 95th percentile men. Since the seat post is fixed when the cycle is manufactured, it is placed at a distance corresponding to the grip reach distance of 5th percentile women. So, everyone can easily reach the handlebar without bending too forward.[14] It is good to design the seat position (front and backward distance) as per adjustable range. This is because if a person has larger grip reach distance and if the seat is fixed as per the distance of 5th percentile women's grip reach, then it would be uncomfortable for a person with greater grip reach as he should bend his elbows laterally. This adjustable seat position is achieved with the help of the rod attached to the bottom of the seat pan and the fixed seat post. The rod slides front and back over the seat post, thus adjusting the horizontal distance between the handlebar and the seat pan.

The grip reach for 5th percentile population is 653.8 mm and for 95th percentile population is 814.2 mm as per anthropometric data.[6] Nearly there is 160 mm difference between each measurement. In general, the seat post distance from the handlebar will be corresponding to the 5th percentile distance (653.8mm). In order to be comfortable even for 95th percentile population, the seat should be 160 mm backward from the seat post. So, the rod of 180 mm (160 mm + 20 mm addendum) is designed and fixed to the bottom of the seat pan and allowed to slide over the fixed seat post. This will be helpful even for a person with a grip reach distance corresponding to the 95th percentile population. They can slide the rod backward to a distance of 160mm and now the seat will be in a position corresponding to a grip reach distance of 95th percentile population (814.2mm).

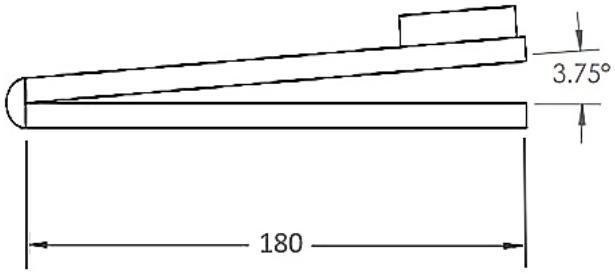

Figure 4: Proposed design of supporting rod

The backrest height should be half of the sitting shoulder height.[4] The sitting shoulder height is 400 mm.[7] Half of that is equal to 200 mm. So, the backrest height should be 200 mm as shown in figure 5.

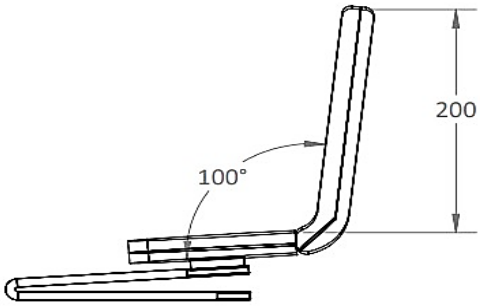

Figure 5: Backrest height and angle

In order to prevent disc pressure, the lumbar spine should promote lumbar lordotic position (spine curved inwards). For this purpose, the backrest angle is inclined backward at an angle of 100^0. The backrest should not be inclined too much i.e.,

more than 110^0 because high inclination of the backrest increases the maximum forward shear force greater than 12%. This leads to skin injuries at the groin.[5]

The cycle backrest width is chosen around two third of the average chest breadth. The average value of chest breadth is 272 mm. Two third of the chest breadth is 180mm. Hence backrest width is taken as 180 mm.

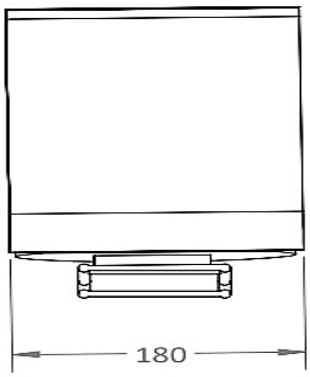

Figure 6: Backrest width

This 180 mm width of backrest covers two third width of the back and provides better support for the lower back. The total backrest thickness is chosen as 25 mm from which the padding of backrest is chosen as 10 mm and the cushioning is chosen as 15 mm. Based on the above mentioned design parameters the seat pan, backrest and the supporting rod are modelled and assembled in 3D modelling software.

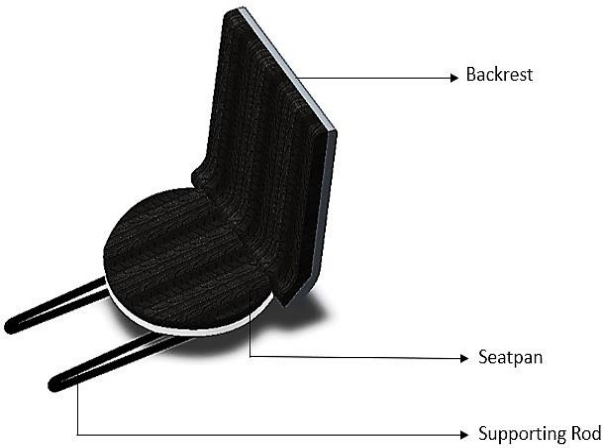

Figure7: Final model of the saddle

The following measurements are found out from the assembly

I. Mass of the assembly = 2.078 kg
II. Surface area of the assembly = 2951.25 cm^2
III. Volume of the assembly = 1452.70 cm^2

The maximum vertical forces during cycling expressed in % Body wight (BW) is found out to be 52% of BW, maximum lateral force during cycling is found out to be 5% of BW and the maximum forward shear force is found out to be 12% of BW.[15] For the design of ergonomic noseless seat, the seat is designed to withstand a maximum of human mass of 120kg (1200 N). So the following loads act on the seat pan for a Bodyweight of 120kg.

I. Maximum vertical load =52% of 1200= 624 N
II. Maximum lateral force = 5 % of 1200 = 60 N
III. Maximum shear force: 12 % of 1200 = 144 N

The lateral seat forces act from left to right and from right to left on the surface of the seat. The lateral force acts from left to right when the pedal crank revolution angle is 0 to 180^0 (when left leg is driving) and right to left when the pedal crank revolution angle is 180 to 360^0 (when right leg is driving).[15] The shear force in this design is regarded as the forward shear force as the seat pan in this design is tilted anteriorly (forward tilt) to an angle of 3.75^0 and the backrest is inclined backwards to an angle of 100^0. This constitutes forward shear force. The maximum shear force is chosen as the maximum value of force during 0 to 180^0 and 180 to 360^0 of pedal crank revolution angle.[16]

As the backrest inclination is increased, the backrest experiences more weight i.e., as backrest angle increases the normal load on the backrest also increases. The thorax and pelvis together applied a normal force to the backrest of 212 N with a standard deviation of 50 N for experiments on 23 men.[16] The 212 N was measured at a backrest angle of 110°. Since our design is for backrest angle of 100^0 only, the normal load on backrest will be less than 212 N (for 110^0 backrest angle). But for safer design the backrest force of 250 N is considered for backrest angle of 100^0 also.

The UPVC/Silica-aerogel composites have better tensile properties, impact strength, hardness and thermal conductivity and the ideal values are referred and mentioned in Table 1.[10,17] Hence the base padding material for seat pan is chosen as UPVC/Silica – Aerogel composite.

Discomfort occurs due to lateral acceleration when cycling. Presence of seat cushion on the padding reduces this discomfort.[18] So seat cushioning material is chosen as Polyurethane foam. Polyurethane flexible foams are widely used for a variety of applications to improve comfort and durability.[19] Aluminum alloy 6061 has high strength and stiffness to weight ratio and may be used for light weight and high strength applications.[20] So the material for backrest padding is chosen as Aluminum alloy 6061.

Stainless steel has excellent qualities in terms of strength and ductility, combined with good corrosion resistance.[21] Hence the material for supporting rod is chosen to be stainless steel.

Table 1: Properties of UPVC/Silica-Aerogel

Property	Unit	Value
Density	kg/m^3	1460
Young's Modulus	MPa	3300
Poisson's Ratio		0.47
Tensile yield Strength	MPa	45 -50
Compressive yield Strength	MPa	59

The analytical validation of the final assembly is carried out using static structural analysis in Ansys Workbench 2022 R2 software. The material assignment for the seat pan, backrest and supporting rod are given as follows.

I. UPVC/Silica-Aerogel is assigned to the padding of seat pan.
II. Polyurethane Foam is assigned to the cushioning of seat pan and backrest.
III. Stainless Steel is assigned to the supporting rod.
IV. Aluminum Alloy 6061 is assigned to the padding of the backrest.

The base of the supporting rod and the edges connecting the backrest and the seat pan are fixed. The Loading conditions at the seat pan and backrest are as follows

I. Maximum vertical load on the seat pan = 624 N
II. Maximum lateral force at seat pan (Both directions) = 60N
III. Maximum Forward shear force at seat pan = 144N
IV. Maximum normal load at the backrest = 250N

Once the boundary conditions and the input force values are assigned, fine meshing is done on the model and the element type chosen is Quadratic Tetrahedral and Quadratic Hexahedral because it is a homogeneous Structural Solid which is well suited to modeling irregular meshes and this element supports multiple shapes. The element size for meshing is given as 10mm.

Results

The maximum stress of 434 MPa occurs on the edge of the supporting rod as shown in figure8. The supporting rod which is a stainless steel has yield strength of 340 MPa. The maximum stress is more than the yield strength. Hence the design fails.

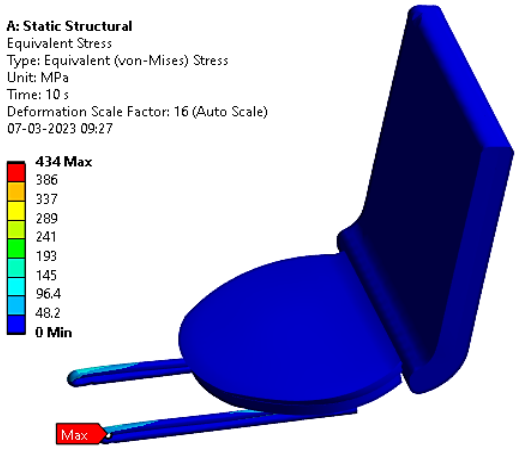

Figure 8: Von Misses Stress when right to left lateral force

The maximum stress of 410 MPa occurs on the edge of the supporting rod. The supporting rod which is a stainless steel has yield strength of 340 MPa. The maximum stress is more than the yield strength. Hence the design fails.

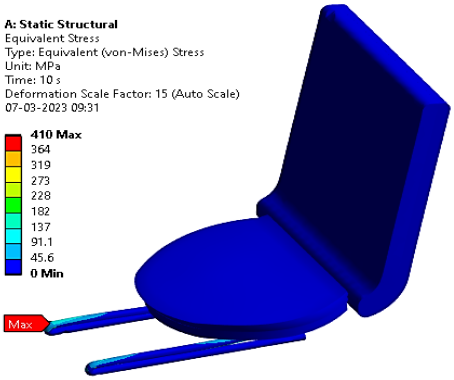

Figure 9: Von Misses Stress when left to right lateral force

The reason for this failure is because there is negligible gap between the end of the supporting rod. This causes more stress at the end of the rod as shown in figure 10. So, the plastic deformation occurs at the edge of the rod.

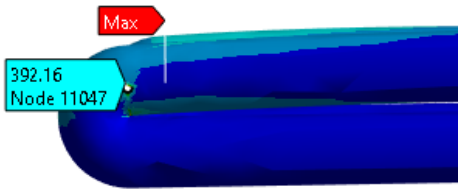

Figure 10: Maximum stress induced at the end of the rod

In order to prevent the failure of the model, the distance between the end of the rods is increased. So, there will not be much stress acting at the end.

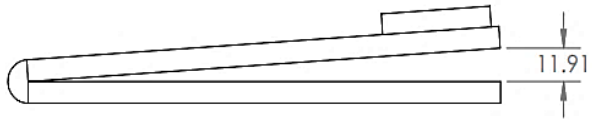

Figure 11A: Failure design

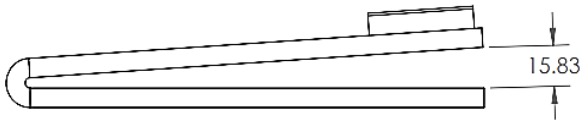

Figure 11B: Corrected Design

Now the supporting rod design is corrected by increasing the gap length from 11.91 mm to 15.83 mm as shown in figure 11A and 11B.

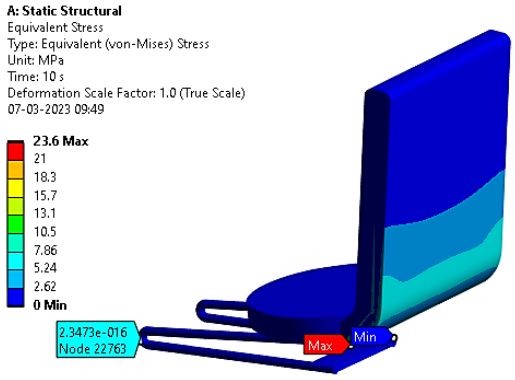

Figure 12: Von Misses Stress after design correction

After design correction, the stress at the gap of supporting rod is negligible because after increase in length of the gap, the upper and lower rod do not interfere when load is applied. So large stress is not caused at end of rod. Also, for aluminum alloy as shown in figure 12, the maximum stress induced is 23.6 MPa which is low compared to its yield strength of 280 MPa.

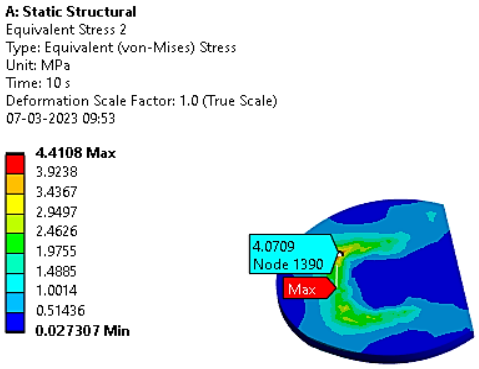

Figure 13: Von Misses Stress for UPVC/Silica-Aerogel padding after design correction

For UPVC/Silica-Aerogel, the maximum stress induced is 4.41 MPa as shown in figure 13 which is low compared to its yield strength of 59 MPa. The stress induced at UPVC /Silica-Aerogel padding is also verified numerically as follows. The saddle stress is caused due to compressive stress when a normal load acts on it. So, the normal load alone is taken into account for compressive stress. When a normal load of 624N is applied to the UPVC/Silica-Aerogel padding, the padding compresses itself with the fixture of the supporting rod and induces a compressive stress.

The compressive stress on the padding is calculated by considering the uniformly distributed load (UDL) actin on the padding and its top surface area.

UDL is nothing but the normal load acting on the padding which is 624 N/mm.

Length of the padding is 130 mm

Top surface area of the padding is 18629.69 mm^2

Equivalent point load for the UDL

= 130 mm * 624 N/mm

= 81120 N

Compressive Stress on padding

= 81120 / 18629.69

= 4.354 MPa

The compressive stress of 4.35 MPa obtained using theoretical calculation is almost satisfied with the result of 4.41 MPa obtained using FEA software. Therefore, it is concluded that the maximum stress induced on the UPVC/Silica-Aerogel padding is less compared to its yield strength and this composite is suitable for using as a padding for seat pan. As all the component's maximum stress is lower than their corresponding yield strengths, the design is considered to be safe.

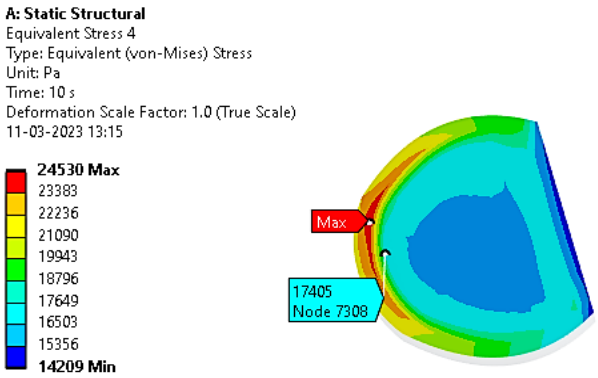

Figure 14: Anterior Saddle pressure at noseless seat

The traditional saddle with nose was associated with an average perineal pressure between 34 kPa and 41 kPa and the noseless saddles were associated with an average perineal pressure of 18 kPa when a person with average weight of 80 kg sits on it.[2] For our proposed design of noseless

anterior curved surface saddle, when a person with 80 kg weight sits, maximum anterior stress is found out to be approximately 24.5 kPa and the average anterior stress is around 17.5 kPa from figure 14. The anterior stress is found out when the following loads act on the seat pan for a Bodyweight of 80 kg (800 N).

I. Maximum vertical load = 52% of 800= 416 N
II. Maximum lateral force = 5 % of 800 = 40 N
III. Maximum shear force: 12 % of 800 = 96 N.

Hence the perineal pressure at noseless seat is lesser compared to that of seat with protruding nose. This lesser perineal pressure at the noseless anterior curved surface saddle reduces the risk of erectile dysfunction, impotence and groin numbness 3 to 4 times than those of traditional saddle with the protruding nose.[2,22] Also this seat shape accommodates upto the sit bone width only and the remaining portion of thighs will be stable to rotate the pedal of the cycle.

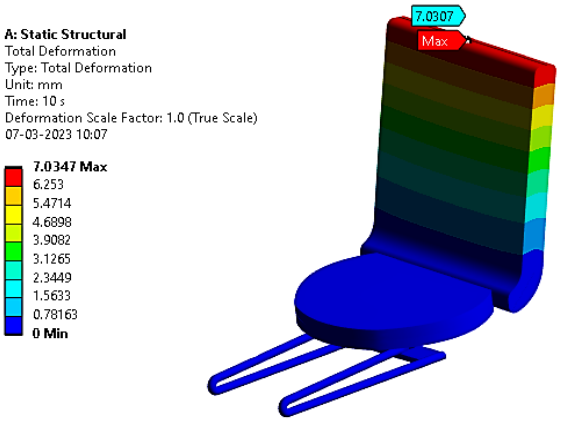

Figure 15: Deformation for UPVC backrest padding

When UPVC/Silica-Aerogel is used for backrest padding, the maximum deformation occurred on the backrest is around 7 mm as shown in figure 15 which is very large and this large deformation causes the failure of joint between backrest and seat pan. In order to overcome the large deformation on the backrest, aluminum alloy 6061 is used as a padding material for the backrest.

When Al alloy is used instead of UPVC for backrest padding, the deformation at the backrest is just 0.38 mm which is negligible. Hence very negligible deformation occurs when Al alloy is used. This is because Al alloy is stronger and has higher density compared to UPVC. Also, the maximum deformation occurs at the anterior edge of the seat pan which is 0.52 mm as shown in figure 16. This deformation is also considered negligible.

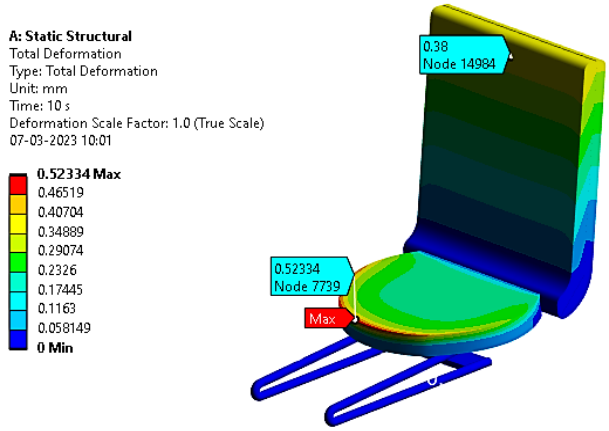

Figure 16: Deformation for Al alloy backrest padding

Discussion

The basic design of noseless bicycle saddle was finalized after the iteration process. Analytical Validation of the model is carried out using an FEA package. Initially the maximum stress induced at the edge of supporting rod which is 434 MPa is greater than its yield strength (340 MPa). So, the design failed initially. Then the gap between the upper and lower edge of the rod is increased from 11.91 mm to 15.83 mm. Now this new model with the corrected design of the supporting rod is analyzed. The maximum stresses induced in the newly proposed material UPVC/Silica-Aerogel and also in other component materials are lesser than their corresponding yield strengths. Now the design is safer and can be proceeded for prototyping. The average perineal stress induced at the anterior edge of the noseless seat which is 17.5 kPa is lesser compared to the anterior stress of saddle with the protruding nose (34 – 41 kPa). This lesser perineal pressure at the noseless anterior curved surface saddle reduces the risk of erectile dysfunction, impotence and groin numbness.[22]

Conclusions

As the anterior saddle stress is reduced, the perineal pressure of the cyclists is highly prevented and this mitigates various health problems associated with the perineal pressure. Also, the inclined backrest inclined enhances the supporting of back muscles and promotes lumbar lordotic position which in turn reduces the disc pressure and low back pain among cyclists. The dynamic analysis of the saddle pressure is not carried out due to lack of experimental and equipment facilities. The experimental research will be executed shortly to conduct the dynamic analysis of the saddle pressure in the future work of study. Thus, the objective of the project is fulfilled.

References

1. Felipe Pivetta Carpes , Frederico Dagnese, Julio Francisco Kleinpaul, Elisandro de Assis Martins, Carlos Bolli Mota. Bicycle saddle pressure: effects of trunk position and saddle design on healthy subjects. Urologia Internationalis. 2009;82:8–11. Available from: https://doi.org/10.1159/000176017

2. Brian D Lowe ,Steven M Schrader, Michael J Breitenstein. Effect of Bicycle Saddle Designs on the Pressure to the Perineum of the Bicyclist. Medicine & Science in Sports & Exercise. 2004 Jun;36(6):1055-62. Available from: https://doi.org/10.1249/01.mss.0000128248.40501.73

3. Mandy Marsden, Martin Schwellnus. Lower back pain in cyclists: A review of epidemiology, pathomechanics and risk factors. International SportMed Journal. 2010;11(1):216-25. Available from: https://www.researchgate.net/profile/Martin-Schwellnus/publication/255897811_Lower_back_pain_in_cyclists_A_review_of_epidemiology_pathomechanics_and_risk_factors/links/559218b108ae15962d8e475d/Lower-back-pain-in-cyclists-A-review-of-epidemiology-pathomechanics-and-risk-factors.pdf

4. Jirapure SC, Andure MW, Mohod SW. Ergonomic Design of a Bicycle-A bike of Rural People. International Journal of Computer Applications. 2012. Available from: https://www.ijcaonline.org/proceedings/efitra/number3/5952-1024

5. Sally L Lusk. Effects of Backrests and Rest Breaks. Sage Journals. 1999;45(12):646-50. Available from: https://doi.org/10.1177/216507999704501204

6. Joydeep Majumder. Anthropometric dimensions among Indian males — A principal component analysis. Eurasian Journal of Anthropology. 2014;5(2):54-62. Available from: https://dergipark.org.tr/en/pub/eja/issue/48765/620439

7. Samuel A Oyewole, Joel M Haight, Andris Freivalds. The ergonomic design of classroom furniture/computer work station for first graders in the elementary school, International Journal of Industrial Ergonomics. Elsevier; 2010;40(4):437-47. Available from: https://doi.org/10.1016/j.ergon.2010.02.002

8. Renato Rodano, Roberto Squadrone, Massimiliano Sacchi, Alberto Marzegan. Saddle pressure distribution in cycling: comparison among saddles of different design and materials. International Society of Biomechanics in Sports. 2002. Available from: https://ojs.ub.uni-konstanz.de/cpa/article/view/806

9. Abraham Mengesha Woldemariam, Walter O Oyawa, Timothy Nyomboi. (2019) Structural Performance of uPVC Confined Concrete Equivalent Cylinders Under Axial Compression Loads. Buildings journal. 2019;9(4):82. Available from: https://doi.org/10.3390/buildings9040082

10. Navid Eskandari, Siamak Motahari, Zhale Atoufi, Ghodratollah Hashemi Motlagh, Mohammad Najafi. Thermal, mechanical, and acoustic properties of Silica-Aerogel/UPVC composites. Journal of applied polymer science. 2016;134(14). Available from: https://doi.org/10.1002/app.44685

11. Yi-Lang Chen, Yi-Nan Liu. Optimal protruding node length of bicycle seats determined using cycling postures and subjective ratings. Applied Ergonomics. Elsevier; 2014;45(4):1181-86 Available from: https://doi.org/10.1016/j.apergo.2014.02.006

12. Mark S Sanders, Ernest J McCormick. Human factors in engineering and design (7th ed). New York: McGraw-Hill, 1970. Available from: https://eprint.ulbi.ac.id/1712/1/Human%20Factor%20In%20Engineering%20And%20Design.pdf

13. Moshe Salai, Tamar Brosh, Alexander Blankstein, Arial Oran, Aharon Chechik. Effect of changing the saddle angle on the incidence of low back pain in recreational bicyclists. British Journal of Sports Medicine. 1999;33(6):398–400. Available from: http://dx.doi.org/10.1136/bjsm.33.6.398

14. Amy Silder, Kyle Gleason, Darryl G Thelen. Influence of Bicycle Seat Tube Angle and Hand Position on Lower Extremity Kinematics and Neuromuscular Control: Implications for Triathlon Running Performance. Journal of Applied Biomechanics. 2011;27(4):297-305. Available from: https://doi.org/10.1123/jab.27.4.297

15. Chisom Wilson, Tamara Reid Bush. Interface forces on the seat during a cycling activity. Clinical Biomechanics. Elsevier; 2007;22(9):1017-23. Available from: https://doi.org/10.1016/j.clinbiomech.2007.06.004

16. Christian G Olesen, Mark de Zee, John Rasmussen. Comparison between a computational seated human model and experimental verification data. Applied Bionics and Biomechanics. 2014;11:175-83. Available from: https://doi.org/10.3233/ABB-140105

17. Vinosh Mani, Navin Kumar Selvaraj, Premkumar Veeraiah, Prassana Jayakumar, Mohammed Saliek Risavu Mydeen. Review of materials and mechanisms used in the conversion of a foldable

chair to a bed. AIP Conference Proceedings 2527. 2022. Available from: https://doi.org/10.1063/5.0108136

18. George F Beard, Michael J Griffin. Discomfort during lateral acceleration: influence of seat cushion and backrest. Applied Ergonomics. Elsevier; 2013;44(4):588-94. Available from: https://doi.org/10.1016/j.apergo.2012.11.009

19. Eniko Mester, Daniel Pecsmany, Karoly Jalics, Adam Filep, Miklos Varga, Kitti Graczer, et al. Exploring the Potential to Repurpose Flexible Moulded Polyurethane Foams as Acoustic Insulators. Polymers. 2022;14(1):163. Available from: https://doi.org/10.3390/polym14010163

20. Shipra Verma. Study on Mechanical Behavior of Aluminum Alloy 6061 Based Composites a Review. IOSR Journal of Mechanical and Civil Engineering. 2018;15(4):16-20. Available from: https://www.researchgate.net/publication/327780602_Study_on_Mechanical_Behavior_of_Aluminum_Alloy_6061_Based_Composites_a_Review/link/5ba40905a6fdccd3cb675664/download

21. Andrea Di Schino. Manufacturing and Applications of Stainless Steels. Metals. 2020;10(3):327. Available from: https://doi.org/10.3390/met10030327

22. James J Potter, Julie l Sauer, Christine l Weisshaar, Darryl G Thelen, Heidi-Lynn Ploeg. Gender differences in bicycle saddle pressure distribution during seated cycling. Medicine & Science in Sports & Exercise. 2008;40(6):1126-34. Available from: https://doi.org/10.1249/MSS.0b013e3181666eea